Microstrip Patch antenna for Wi-Fi and 5G based on MUC

Suman Nelaturi (nelaturi.suman4@gmail.com)
Vignan's Foundation for Science Technology and Research https://orcid.org/0000-0002-4820-7524

Research Article

Keywords: Dual band, Mushroom Unit Cell, Double Negative Transmission line

Posted Date: December 2nd, 2022

DOI: https://doi.org/10.21203/rs.3.rs-190468/v1

Microstrip Patch antenna for Wi-Fi and 5G based on MUC

Suman Nelaturi

Department of ECE, Vignan's Foundation for Science Technology and Research (Deemed to be university), Guntur, AP, India.

nelaturi.suman4@gmail.com

Abstract: This communication presented the patch antenna functioning at Wi-Fi and 5G bands. To get compactness the side lengths of the patch are calculated with reference to upper-frequency band (3.5 GHz). Lower band (2.4 GHz) is obtained by loading the Mushroom Unit Cell (MUC) along the bottom right corner of the patch. To attain circular polarization (CP) at 5G band the edges of the patch are replaced with Koch fractal curves. This blend of the Double Negative Transmission Lines metamaterials (DNG TL), as well as fractal concepts yielded good compactness suitable for ultra-thin portable gadgets. Measured results have good correlation with simulated data from HFSS. The achieved bandwidths at the lower and upper bands are 2.4% and 5.6%. CP bandwidth of the proposed antenna at 5G band obtained from the measured data is 2.2%.

Keywords: Dual band, Mushroom Unit Cell, Double Negative Transmission line

Introduction:

Artificial materials like Metamaterials are best alternative for designing thin and compact antennas because of their special electromagnetic properties [1]. These materials will support backward wave propagation, due to which left-handed bands (zeroth order or negative order modes) are produced. Metamaterials or left-handed materials are categorized into ENG materials, MNG materials and DNG materials. Metamaterials are constructed using VIAs, Split Ring Resonators (SRRs). The pioneers in this area analyzed the Metamaterials based on transmission line theory [2]. Dual band or multi band antennas based on MUC are proposed in [3- 10], based on CSRR are presented in [11- 15] and based EBG are listed in [16- 20]. Dual band dual polarised antenna is reported in [21]. All these antennas are suffering from the size and resonating frequency ratio ie. Lower resonating frequency occurs at the cost of the large volume of the patch. But the proposed antenna is able to produce a lower resonating band for lower dimensions of the patch.

In this article, patch antenna functioning at Wi-Fi and 5G bands is endeavored. CP at patch mode is achieved by providing asymmetry to the patch through the fractal curves embedded along the length and width of patch. Simulations are conducted in Ansoft HFSS.

Structure of reported antenna

The suggested antenna structure is specified in Fig. 1. Described antenna is implemented on dielectric material (Rogers RT/Duroid) has ϵ=2.2, h=3.175 mm. Radiating patch is slotted at the right bottom corner to load MUC. The dimensions of the slot are 10x10 mm^2. Square MUC having a metallic patch with a side length of 9.5 mm and a VIA with 0.3 mm radius is loaded into the patch. The series capacitance due to the gap between patch and MUC and shunt inductance due to VIA are the main cause of getting zeroth order band (left-hand band). The physical parameters of presented antenna are listed in Table 1.

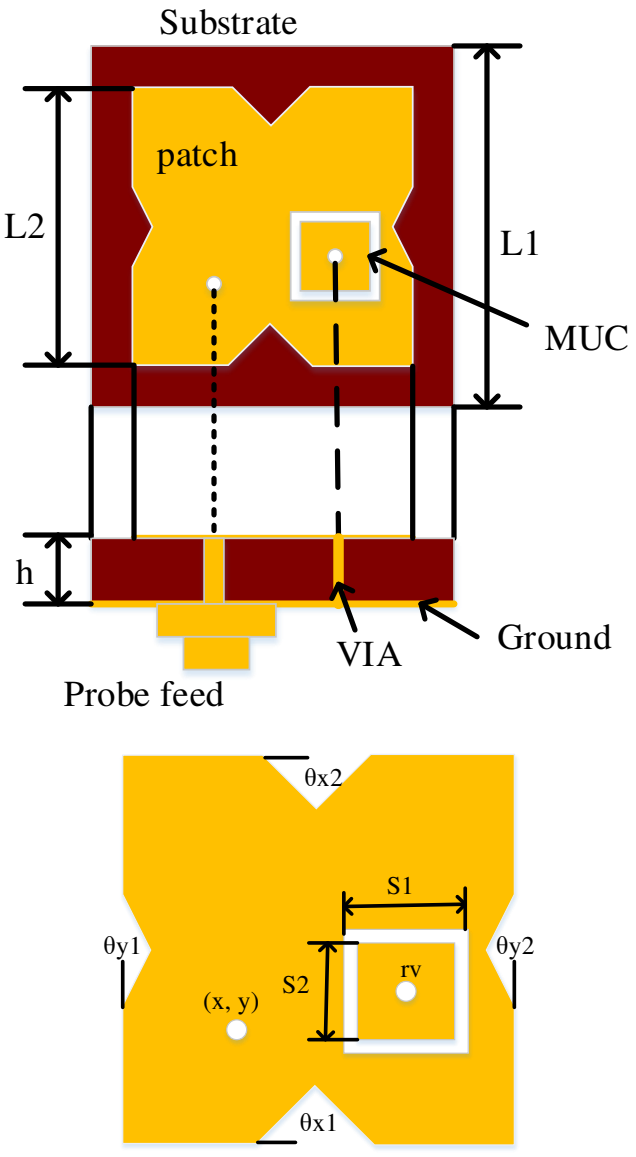

Fig. 1 a proposed antenna structure

Table 1: parameter values

Parameter	L_1	L_2	S_1	S_2	θx1=θx2	θy1=θy2	h	r_v
Value in mm	36	26	10	9.5	60^0	30^0	3.175	0.3

DNG TL theory and Simulation Results

DNG TL unit cell equivalent circuit is stated in Fig.2, where L_R and C_R are series inductance and shunt capacitance per unit length in which both are due to patch and L_L is the shunt inductance due to VIA and C_L is series capacitance due to the gap between radiating patch and MUC.

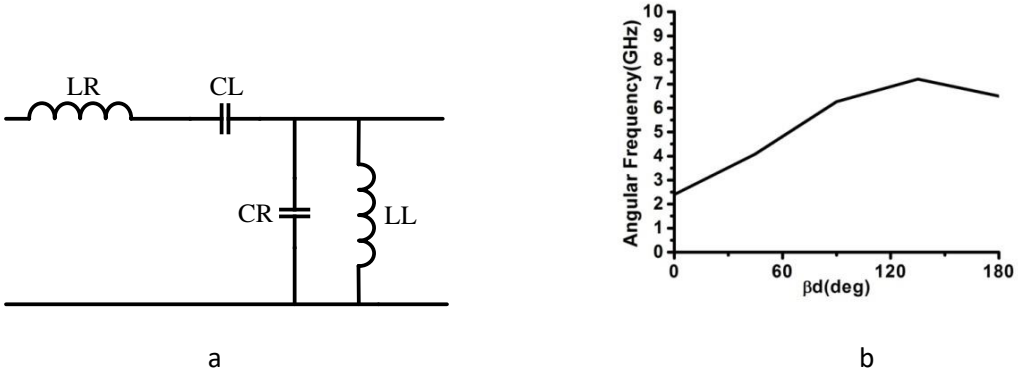

Fig. 2 DNG TL unit cell a Equivalent circuit diagram b dispersion characteristics plot

The relationship between the phase constant and the angular frequency is obtained by using Bloch Floquet theory. According to them the propagation constant of DNG TL is given by

$$\gamma = \sqrt{ZY} \quad . \qquad (1)$$

Where Z is the series impedance and Y is the shunt admittance and they are given by

$$Z = jwL_R - \frac{j}{wC_L}$$

$$Y = jwC_R - \frac{j}{wL_L}$$

We know that propagation constant is the combination of attenuation constant and phase constant as shown below

$$\gamma = \alpha + j\beta \qquad (2)$$

Therefore $\alpha + j\beta = \sqrt{ZY}$

$$\alpha + j\beta = \sqrt{ZY} = \sqrt{(jwL_R - \frac{j}{wC_L})(jwC_R - \frac{j}{wL_L})}$$

$$\alpha + j\beta = \sqrt{ZY} = \sqrt{-w^2 L_R C_R + \frac{L_R}{L_L} + \frac{C_R}{C_L} - \frac{1}{w^2 L_L C_L}}$$

Let $w_R = \frac{1}{\sqrt{L_R C_R}}$ $w_{sh} = \frac{1}{\sqrt{L_L C_R}}$

$w_{se} = \frac{1}{\sqrt{L_R C_L}}$ $w_L = \frac{1}{\sqrt{L_L C_L}}$

$$\alpha + j\beta = \sqrt{ZY} = \sqrt{\frac{-w^2}{w_R^2} + \frac{w_L^2}{w_{se}^2} + \frac{w_L^2}{w_{sh}^2} - \frac{w_L^2}{w^2}}$$

$$\alpha + j\beta = \sqrt{ZY} = j * \sqrt{\frac{w^2}{w_R^2} - \frac{w_L^2}{w_{se}^2} - \frac{w_L^2}{w_{sh}^2} + \frac{w_L^2}{w^2}}$$

$$\cosh(\alpha + j\beta) = \cosh(j * \sqrt{\frac{w^2}{w_R^2} - \frac{w_L^2}{w_{se}^2} - \frac{w_L^2}{w_{sh}^2} + \frac{w_L^2}{w^2}})$$

$$\cosh\alpha\cos\beta + j\sinh\alpha\sin\beta = (2 + j^2 * (\frac{w^2}{w_R^2} - \frac{w_L^2}{w_{se}^2} - \frac{w_L^2}{w_{sh}^2} + \frac{w_L^2}{w^2}))/2$$

We know that for a lossless transmission line, the attenuation constant α =0

$$\cos\beta = 1 - 0.5 * (\frac{w^2}{w_R^2} - \frac{w_L^2}{w_{se}^2} - \frac{w_L^2}{w_{sh}^2} + \frac{w_L^2}{w^2})$$

Therefore the phase constant β is given by

$$\beta = \arccos(1 - 0.5 * (\frac{w^2}{w_R^2} - \frac{w_L^2}{w_{se}^2} - \frac{w_L^2}{w_{sh}^2} + \frac{w_L^2}{w^2})) \quad (3)$$

From the above equation, it is observed that the phase constant is dependent on four different angular frequencies. Those are patch mode frequency (w_R) or n=+1 mode, zeroth order frequency (w_{sh}) or n=0 mode, w_{se} or n=-1 mode and w_L or n=+2 mode respectively. The proposed antenna is resonating at two frequencies only those are patch mode band and zeroth order band. The phase constant is negative for n=0 mode and positive for the n=+1 mode. The dispersion characteristics plot of the reported antenna is shown in Fig. 2, which gives the information about zeroth order resonant (ZOR) frequency. Here the ZOR is at 2.4 GHz which is independent of the wavelength of the patch (the ZOR frequency occurred at infinite wavelength which is the speciality of the DNG TL).

The design and development of the reported antenna is given in Fig. 3. At first, the square patch Ante1 is designed for 5G band (3.3 GHz) where the polarization is linear. The CP at this single band can be obtained by replacing edges of the square patch with Poly fractal

curves which results in Ante2. Ante3 is achieved by inserting MUC along the bottom right corner of Ante1 to produce two bands with LP. Finally, Ante4 can be designed by loading MUC in Ante2 to result in dual-band patch antenna with first band LP and the second band with CP. The optimized feed point location is obtained from the software tool which is 4.5 mm distance away diagonally from the patch center position. Simulated Return Loss (RL) properties of presented antenna are given in Fig. 4.

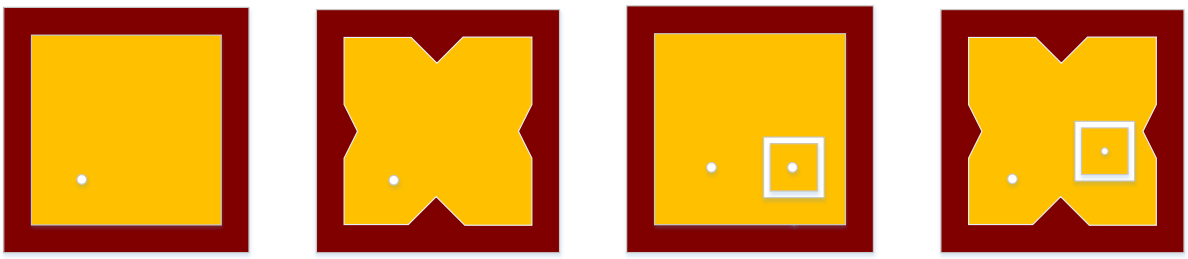

Ante1 Ante2 Ante3 Ante4

Fig. 3 In between steps in the design

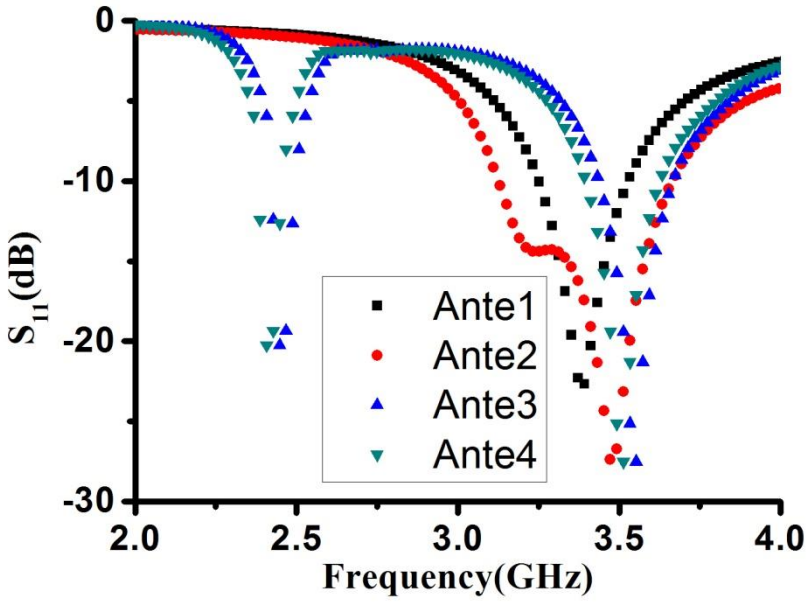

Fig. 4 Simulated RL characteristics

Table 2: Impedance bandwidth values

S. No	Antenna	Impedance bandwidth (%)	
		Band1	Band2
1	Ante1	-----	7.69% (3.25- 3.51 GHz)
2	Ante2	-----	12.38% (3.13- 3.65 GHz)
3	Ante3	2.44% (2.42- 2.48 GHz)	5.63% (3.45- 3.65 GHz)
4	Ante4	2.48% (2.38- 2.44 GHz)	5.69% (3.41- 3.61 GHz)

From fig. 5, it is observed that, if the dimensions of the square MUC are decreasing, then the left-hand band is moving from left side to right side on the frequency scale. The dimensions of the MUC are optimized (S2= 9.5 mm) to get the left-hand band exactly at 2.4 GHz.

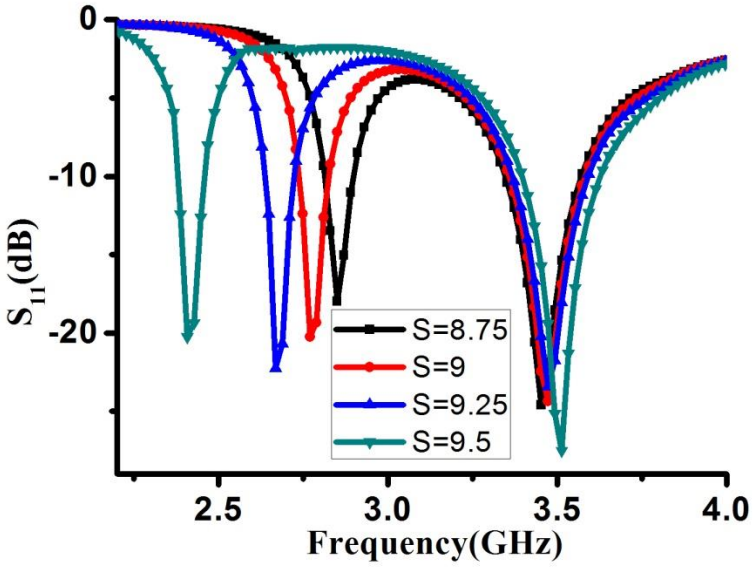

Fig. 5 Optimized RL characteristics

To interpret the working mechanism of reported antenna, simulated surface current distributions at each frequency band are given in the Fig. 6. The cause for Wi-Fi band (2.4 GHz) is current distribution across MUC. 5G band (3.5 GHz) is because of strong surface current at sides of fractal patch.

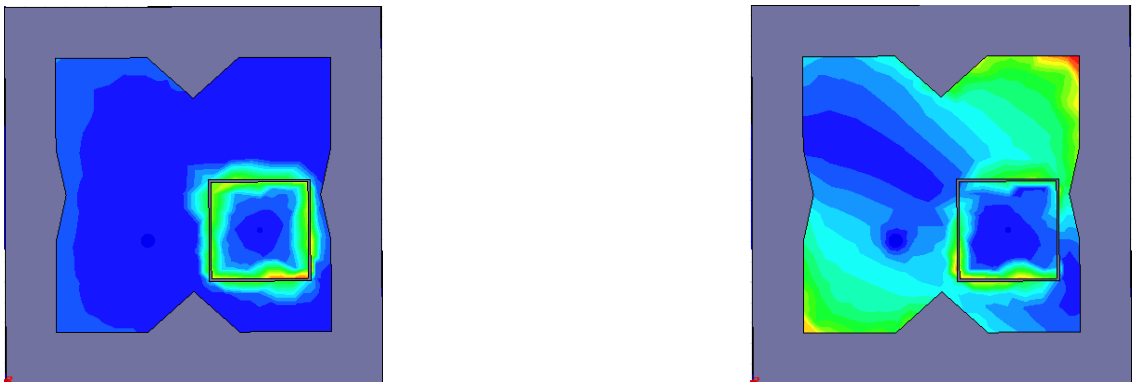

a b

Fig. 6 Surface current at a Wi-Fi band (2.4 GHz) b 5G band (3.3 GHz)

Experimental Results

The demonstrated antenna (Ante4) is manufactured with dielectric material (Rogers RT/Duroid) has dimensions 37 x 37 x 3.175 mm^3 as shown in Fig. 7. The MUC is loaded into the patch. Return Loss properties are measured using Agilent 8719A microwave network

analyzer. Radiation patterns are obtained from an anechoic chamber with size of 22.5 x 12.5 x 11.5 m^3. The working frequency of chamber is from 400 MHz to 18 GHz.

Top view Bottom view

Fig: 7 prototype of Ante4

Return loss characteristics of Ante4 are shown in the Fig. 8. Experimental results are highly correlated with simulated data. Experimental return loss bandwidth of Poly fractal boundary patch antenna is 2.51% at Wi-Fi band and 6.23% at 5G band respectively. The measured AR plot is given in Fig. 9. AR bandwidth at 5G band is 2.35%. Fig 10 & 11 represent radiation patterns at Wi-Fi and 5G bands. Fig. 12 describes the gain plot.

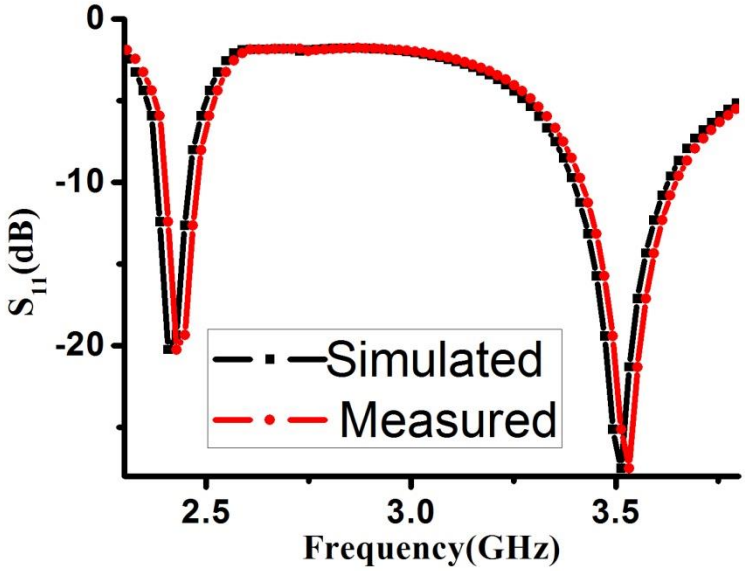

Fig. 8 RL characteristics

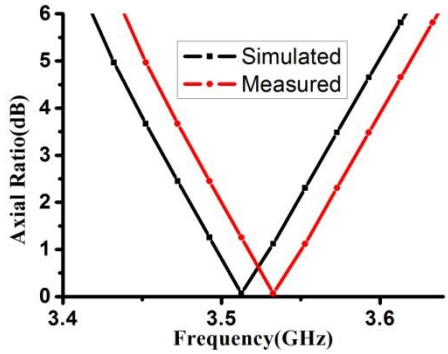

Fig. 9 AR characteristics

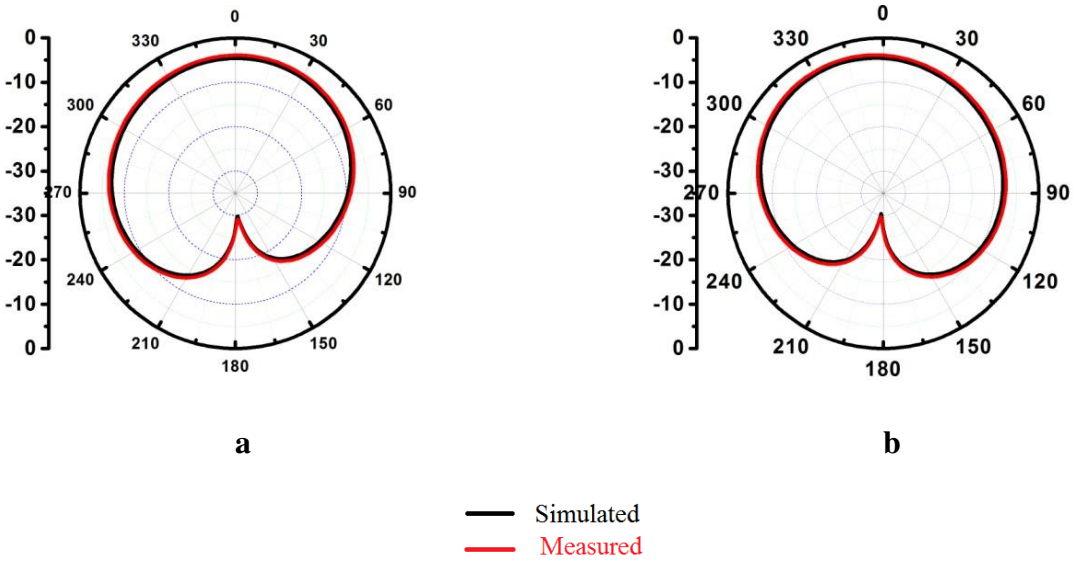

Fig. 10 Radiation pattern at Wi-Fi band a E plane b H plane

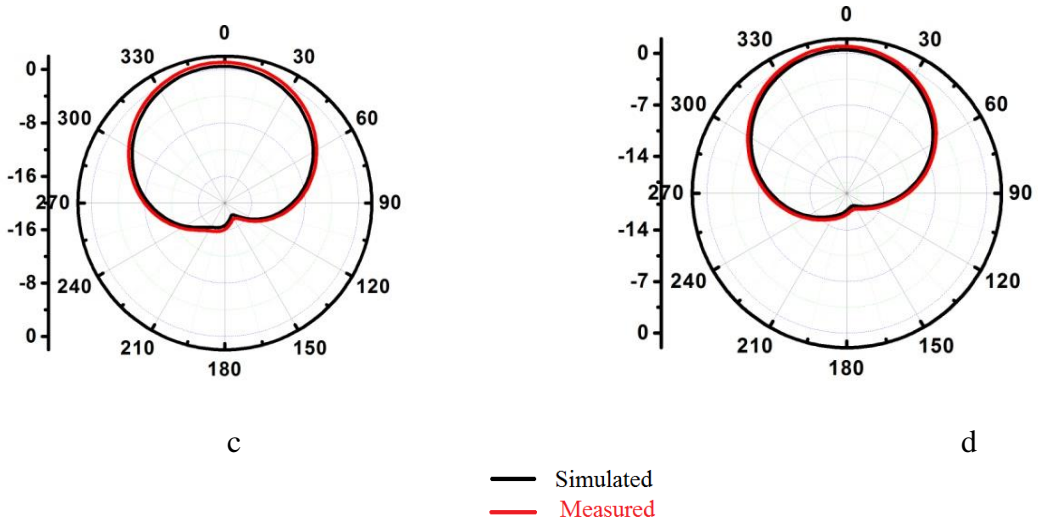

Fig. 11 Radiation pattern at 5G band a E plane b H plane

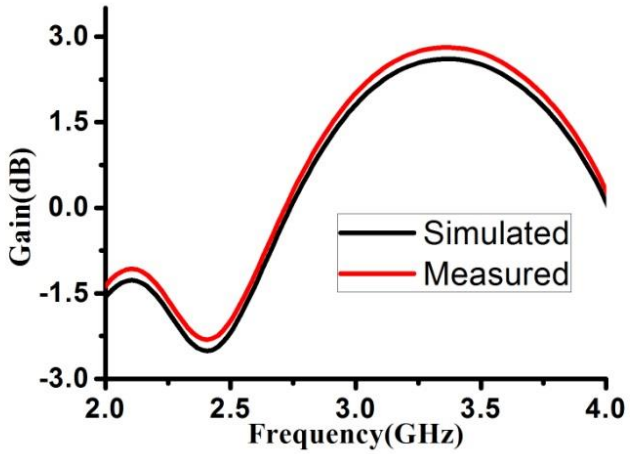

Fig. 12 Gain plot of reported antenna

The comparison between proposed antenna and the antennas in the existing literature is given in Table 3. The antennas presented in [5, 7, 8] are small in size but suffering from bandwidth and gain at operating frequencies.

Table 3 comparison

Antenna	Patch Size (mmxmm)	Substrate size (mmxmmxmm)	10- dB return loss bandwidth at corresponding centre frequency	
			At ZOR	At patch mode
Proposed antenna	26x26	36x36x3.175	2.4% at 2.4 GHz	5.66% at 3.5 GHz
[4]	28.8x28.8	60x60x1.6	3.50% at 2.3 GHz	1.96% at 2.56 GHz
[5]	16x16	36x36x1.5	1.44% at 2.76 GHz	3.05% at 5.23 GHz
[7]	18x18 RIS based	35x35x3	2.59% at 2.4 GHz	8.40% at 3.4 GHz
[8]	26.1x31	26.1x31x1.6	2.4% at 2.5 GHz	8.7% at 2.92 GHz
[13]	27x27	37x37	Resonance at 2.4 GHz only	8.22% at 3.08 GHz

Conclusion

The patch antenna working at Wi-Fi and 5G bands is conveyed in this communication. By optimizing the dimensions of the MUC, feed point and Koch fractal curves, dual-band operation with wide bandwidth is achieved. Return loss bandwidth of the proposed antenna is 2.4% at Wi-Fi band and is 5.66% at 5G band. The 3- dB AR bandwidth is 2.2% at the upper resonating band.

Declarations

Funding

Not applicable

Conflicts of interest/Competing interests

No

Availability of data and material

No

Code availability

No

Authors' contributions

The author confirms sole responsibility for the following: study conception and design, data collection, analysis and interpretation of results, and manuscript preparation.

References

1. Caloz, Christophe, and Tatsuo Itoh. Electromagnetic metamaterials: transmission line theory and microwave applications. John Wiley & Sons, 2005.
2. Park, Jae-Hyun, et al. "Epsilon negative zeroth-order resonator antenna." *IEEE Transactions on Antennas and Propagation* 55.12 (2007): 3710-3712.
3. Amani, Navid, and Amir Jafargholi. "Zeroth-Order and TM_{10} Modes in One-Unit Cell CRLH Mushroom Resonator." *IEEE Antennas and Wireless Propagation Letters* 14 (2015): 1396-1399.
4. Saurav, Kushmanda, Debdeep Sarkar, and Kumar Vaibhav Srivastava. "Dual-polarized dual-band patch antenna loaded with modified mushroom unit cell." *IEEE Antennas and Wireless Propagation Letters* 13 (2014): 1357-1360
5. Zong, Binfeng, Guangming, wand., Cheng, Zhou., Yawai, Wang. "Compact low-profile dual-band patch antenna using novel TL-MTM structures." *IEEE Antennas and Wireless Propagation Letters* 14 (2015): 567-570.
6. El-Raouf, Abd, E. Hany, and Sulaiman Syed Zaheer. "Design of small planar antennas based on double-layered CRLH metamaterials." *Microwave and Optical Technology Letters* 54, no. 10 (2012): 2224-2229.
7. Nelaturi, Suman, and Nookala Venkata Satya Narasimha Sarma. "A compact microstrip patch antenna based on metamaterials for Wi-Fi and WiMAX applications." Journal of Electromagnetic Engineering and Science 18.3 (2018): 182-187.

8. Abdalla, Mahmoud A. "A high selective filtering small size/dual band antenna using hybrid terminated modified CRLH cell." Microwave and Optical Technology Letters 59.7 (2017): 1680-1686.
9. Singh, Amit Kumar, Mahesh P. Abegaonkar, and Shiban K. Koul. "Highly miniaturized dual band patch antenna loaded with metamaterial unit cell." Microwave and Optical Technology Letters 59.8 (2017): 2027-2033.
10. Zhang, Chaoqun, Jianqiang Gong, and Yuhao Wang. "A miniaturized dual band microstrip patch antenna using a symmetrical composite right/left handed unit." Microwave and Optical Technology Letters 59.12 (2017): 3069-3073.
11. Singh, Gautam Kumar, Raghvendra Kumar Chaudhary, and Kumar Vaibhav Srivastava. "A compact zeroth order resonating antenna using complementary split ring resonator with mushroom type of structure." *Progress In Electromagnetics Research Letters*28 (2012): 139-148.
12. Yue, Taiwei., Zhi, Jiang., Anastasios, Panaretos., Douglas, Werner. "A Compact Dual-Band Antenna Enabled by a Complementary Split-Ring Resonator-Loaded Metasurface." *IEEE Transactions on Antennas and Propagation* 65.12 (2017): 6878-6888.
13. Nelaturi, Suman, and N. V. S. N. Sarma. "CSRR based patch antenna for Wi-Fi and WiMAX Applications." Advanced Electromagnetics 7.3 (2018): 40-45.
14. Rajkumar, Rengasamy, and Usha Kiran Kommuri. "A Triangular Complementary Split Ring Resonator Based Compact Metamaterial Antenna for Multiband Operation." Wireless Personal Communications 101.2 (2018): 1075-1089.
15. Pandey, Ganga Prasad, et al. "CSRR loaded tunable L-strip fed circular microstrip antenna." Wireless personal communications 74.2 (2014): 717-730.
16. Velan, Sangeetha, et al. "Dual-band EBG integrated monopole antenna deploying fractal geometry for wearable applications." *IEEE Antennas and Wireless Propagation Letters* 14 (2015): 249-252.
17. Liu, Zhen-Guo, and Yong-Xin Guo. "Compact low-profile dual band metamaterial antenna for body centric communications." *IEEE Antennas and Wireless Propagation Letters* 14 (2015): 863-866.
18. Ali, Mohamed., Adel, Abdel-Rahman., Ahmed, Allam., Hala, Elsadek., Ramesh, Pokharel. "Design of Dual Band Microstrip Antenna with Enhanced Gain for Energy Harvesting Applications." *IEEE Antennas and Wireless Propagation Letters* (2017).
19. Zhang, Shuai. "Novel dual band compact his and its application of reducing array in band RCS." Microwave and Optical Technology Letters 58.3 (2016): 700-704.
20. Sui, Sai, et al. "Multiform frequency selective surfaces optimal design based on topology optimization." International Journal of RF and Microwave Computer Aided Engineering 29.1 (2019): e21491.
21. Kumar, Rajkishor, and Raghvendra Kumar Chaudhary. "A dual band dual polarized cubical DRA coupled with new modified cross shaped slot for ISM (2.4 GHz) and Wi-MAX (3.3-3.6 GHz) band applications." International Journal of RF and Microwave Computer Aided Engineering 29.1 (2019): e21449.